Status on Bidimensional Dark Energy Parameterizations Using SNe Ia JLA and BAO Datasets

Celia Escamilla-Rivera,^a

^aMesoamerican Centre for Theoretical Physics, Universidad Autónoma de Chiapas, Carretera Zapata Km. 4, Real del Bosque (Terán), Tuxtla Gutiérrez 29040, Chiapas, México

E-mail: cescamilla@mctp.mx

Abstract. Using current observations of forecast type Ia supernovae (SNe Ia) Joint Lightcurve Analysis (JLA) and baryon acoustic oscillations (BAO), in this paper we investigate six bidimensional dark energy parameterizations in order to explore which has more constraining power. Our results indicate that for parameterizations that contain z^2 -terms, the tension (σ -distance) between these datasets seems to be reduced and their behaviour is $<1\sigma$ compatible with the concordance model (Λ CDM). Also, the results obtained by performing their Bayesian evidence show a striking evidence in favour of the Λ CDM model, but only one parameterization can be distinguished by around 1% from the other models when the combination of datasets are considered.

\mathbf{C}	ontents					
1	1 Introduction					
2	Modeling dark energy					
3	Bidimensional dark energy parameterizations	2				
	3.1 Lambda Cold Dark Matter-redshift parametrization (ACDM)	2				
	3.2 Linear-redshift parametrization	3				
	3.3 Chevallier-Polarski-Linder parametrization (CPL)	3				
	3.4 Barboza-Alcaniz parameterization (BA)	3				
	3.5 Low Correlation parameterization (LC)	3				
	3.6 Jassal-Bagla-Padmanabhan parametrization (JBP)	4				
	3.7 Wetterich-redshift parameterizations (WP)	4				
4	Observational Data	4				
	4.1 Analysis using SNe Ia data	5				
	4.2 Analysis using BAO data	5				
5	Bayesian Evidence	6				
6	Results					
	6.1 About the Likelihood and Tension	7				
	6.2 About the Figure of Merit (FoM)	7				
	6.3 About the Bayesian Evidence	8				
7	Conclusions	8				

1 Introduction

A highlight in observational cosmology is the origin of the accelerated expansion of the universe. The standard cosmological model that is consistent with current cosmological observations is the concordance model or Λ CDM. According to this framework, the observed accelerating expansion is attributed to the repulsive gravitational force of a cosmological constant Λ with constant energy density ρ and negative pressure p. Despite its simplicity, this standard model has a couple of theoretical loopholes (e.g., the fine tuning and coincidence problems) [1, 2], which had lead to alternative proposals that either modified the General Relativity or consider a scenario with a dynamical dark energy. At this point, dark energy can be described by a parametrized equation of state (EoS) written in terms of the redshift, w(z). Since its properties are still under-researched, several proposals on dark energy parameterizations have been discussed in the literature (see, e.g., [3–9]).

The study of the constraints on the EoS parameter(s) has been done using observables such as: supernovae, baryon acoustic oscillations (BAO), cosmic microwave background (CMB), weak lensing spectrum, etcetera. The importance of using these compilations is due to the precision with which dark energy can be fathomed. Currently, some measurements such as the Joint Lightcurve Analysis (JLA) from supernovae [10, 11], BOSS [12], just to cite a few, point out a way to constrain these EoS parameters. These observations allow

deviations from the Λ CDM model, which are usually parametrized by a bidimensional form (w_0, w_a) .

The aim of this paper is to study six bidimensional dark energy parameterizations, testing them with the SNe Ia and BAO data available and explore which one has more constraining power. The organization of this paper is as follows. In Section 2 we present how to model a parametrized dark energy via its EoS. In Section 3 we review six bidimensional dark energy parameterizations. The astrophysical compilations to be use are described in Section 4. A description of the Bayesian model selection is presented in Sections 5 and 6 we discuss our main results related to the *tension*, the Figure of Merit and the Bayesian evidence for each dark energy parameterization. Our final comments are presented in Section 7.

2 Modeling dark energy

In order to achieve the observed cosmic acceleration, we require an energy density with significant negative pressure at late times. This means that the ratio between the pressure and energy density is negative, i.e., $w(z) = P/\rho < 0$. All reasonable fitting dark energy models are in agreement at this point.

We start with the Friedmann and Raychaudhuri equations for a spatially flat universe

$$E(z)^{2} = \left(\frac{H(z)}{H_{0}}\right)^{2} = \frac{8\pi G}{3}(\rho_{m} + \rho_{DE})\left[\Omega_{0m}(1+z)^{3} + \Omega_{0(DE)}f(z)\right]$$
(2.1)

and

$$\frac{\ddot{a}}{a} = -\frac{H^2}{2} \left[\Omega_m + \Omega_{DE} (1 + 3w) \right]$$
 (2.2)

where H(z) is the Hubble parameter, G the gravitational constant and the subindex 0 indicates the present-day values for the Hubble parameter and matter densities. The energy density of the non-relativistic matter is $\rho_m(z) = \rho_{0m}(1+z)^3$. And the dark energy density $\rho_{DE}(z) = \rho_{0(DE)}f(z)$, where $f(z) = exp[\left[3\int_0^z \frac{1+w(\tilde{z})}{1+\tilde{z}}d\tilde{z}\right]]$.

We notice that modeling w(z) can give directly a description of the $E(z)^2$ function, as e.g., in the case of quiessence models (w = const.) the solution of f(z) is $f(z) = (1+z)^{3(1+w)}$. If we consider the case of the cosmological constant (w = -1) then f = 1. Other cases explore a dark energy density ρ_{DE} with varying and non-varying w(z) (see, e.g., [4, 13] and references therein).

3 Bidimensional dark energy parameterizations

In this section, we present the evolution of $E(z)^2$ for six bidimensional dark energy parameterizations most commonly used in the literature and we identify the parameters to be fitted using the current astrophysical data available.

3.1 Lambda Cold Dark Matter-redshift parametrization (\(\Lambda\)CDM)

Even though our first model has one independent parameter, Ω_m , we shall take it into account to compare with the bidimensional proposals. This model is given by:

$$E(z)^{2} = \Omega_{m}(1+z)^{3} + (1-\Omega_{m})$$
(3.1)

where we consider w = -1.

As it is well known in the literature, this standard model provides a good fit for a large number of observational data compilations without addressing some important theoretical problems, such as the cosmic coincidence and the fine tuning of the Λ value [14].

3.2 Linear-redshift parametrization

The dark energy EOS for this case was presented in [15, 16] and is given by:

$$w(z) = w_0 - w_1 z (3.2)$$

which can be reduced to ΛCDM model (w(z) = w = -1) for $w_0 = -1$ and $w_1 = 0$ Inserting Equation (3.2) into f(z), we obtain

$$E(z)^{2} = \Omega_{m}(1+z)^{3} + (1-\Omega_{m})(1+z)^{3(1+w_{0}+w_{1})} \times e^{-3w_{1}z}$$
(3.3)

However, this ansatz diverges at high redshift and consequently yields strong constraints on w_1 in studies involving data at high redhisfts, e.g., when we use CMB data [17].

3.3 Chevallier-Polarski-Linder parametrization (CPL)

A simple parameterization that shows interesting properties [18, 19] and, in particular, can be represented by two parameters that exhibit the present value of the EoS w_0 and its overall time evolution w_1 is the CPL model, written as:

$$w(z) = w_0 + \left(\frac{z}{1+z}\right)w_1\tag{3.4}$$

The evolution for this parameterization is given by:

$$E(z)^{2} = \Omega_{m}(1+z)^{3} + (1-\Omega_{m})(1+z)^{3(1+w_{0}+w_{1})} \times e^{-\left(\frac{3w_{1}z}{1+z}\right)}$$
(3.5)

3.4 Barboza-Alcaniz parameterization (BA)

Proposed in [20], this model brings a step forward in redshift regions where the CPL parameterization cannot be extended to the entire history of the universe. Its functional form is given by:

$$w(z) = w_0 + \frac{z(1+z)}{1+z^2}w_1 \tag{3.6}$$

which is well-behaved at $z \to -1$. The evolution of this model can be written as:

$$E(z)^{2} = \Omega_{m}(1+z)^{3} + (1-\Omega_{m})(1+z)^{3(1+w_{0})} \times (1+z^{2})^{3w_{1}/2}$$
(3.7)

3.5 Low Correlation parameterization (LC)

In [8] it was proposed a two parameter EoS for the dark energy component, linear in the scale factor and given by:

$$w(z) = \frac{(-z + z_c)w_0 + z(1 + z_c)w_c}{(1 + z)z_c}$$
(3.8)

where $w_0 = w(z = 0)$ and $w_c = w(z = z_c)$. The subindex c is used to indicate the scale factor (or redshift) value for which the parameters (w_0, w_c) are uncorrelated. This value depends on the different used data set. In this model was proposed to fix it at the value $z_c = 0.5$ being this value sufficiently close to the current data value $(z_c \sim 0.3)$ and thus arguing that the correlation between (w_0, w_c) is relatively small. With this value for a_c , the evolution now becomes

$$E(z)^{2} = \Omega_{m}(1+z)^{3} + (1-\Omega_{m})(1+z)^{3(1-2w_{0}+3w_{0.5})} \times e^{\left[\frac{9(w_{0}-w_{0.5})z}{1+z}\right]}$$
(3.9)

The pivot $w_{0.5}$ is a conservative choice which achieved a low degree of correlation and provides a simple expression.

3.6 Jassal-Bagla-Padmanabhan parametrization (JBP)

In [9] another problem in CPL parametrization at high redshift z was addressed. To alleviate this behaviour, the authors proposed a new parametrization with the form

$$w(z) = w_0 + \frac{z}{(1+z)^2} w_1 \tag{3.10}$$

which can present a dark energy component with the same values at lower and higher redshifts, with rapid variation at low z. Combining Equation (3.10) and f(z) we obtain

$$E(z)^{2} = \Omega_{m}(1+z)^{3} + (1-\Omega_{m})(1+z)^{3(1+w_{0})}e^{\frac{3w_{1}z^{2}}{2(1+z)^{2}}}$$
(3.11)

3.7 Wetterich-redshift parameterizations (WP)

Another bidimensional parameterization was proposed in [21], which include the possibility that dark energy contributes to the total energy of the universe to some extent at an earlier epoch. Its form is given by:

$$w(z) = \frac{w_0}{\left[1 + w_1 \ln(1+z)\right]^2}$$
(3.12)

where w_1 is called bending parameter and characterized the redshift where an approximately constant EoS turns over to a different behaviour.

Using Equation (3.12) in f(z) we obtain the following evolution

$$E(z)^{2} = \Omega_{m}(1+z)^{3} + (1-\Omega_{m})(1+z)^{3\left[1 + \frac{w_{0}}{1+w_{1}\ln(1+z)}\right]}$$
(3.13)

We may argue that the form of Equation (3.12) is not general enough and, in particular, not suitable for the description change of sign of w(z). In fact, for typical models with early dark energy we expect w(z) > 0 in the radiation era. However, this ansatz has some corrections when radiation becomes important [22].

4 Observational Data

It is quite strongly stablished that dark energy domination began somewhat recently, and therefore low redshift data, are precisely those best suited for its analysis. The two main astrophysical tools of such nature are the standard candles (objects with well determined intrinsic luminosity) and standard rulers (objects with well determinate comoving size). Such probes provide us with distance measures related to H(z), and the best so far representatives

of those two classes are SNe Ia and BAO. Those are in fact low redshift datasets, and much effort is begin done in those two observational contexts toward obtaining more and better measurements.

On one hand, SNe Ia are extremely rare astrophysical events, the modern and specifically planned strategies of detection make it possible to observe and collect them up to relatively high redshift ($z \approx 2$). On the other hand, the main techniques that rest on the BAO peaks detection in the galaxy power spectrum are promising standard rulers for cosmology, potentially enabling precise measurements of the dark energy parameters with a minimum of systematic errors.

In the following lines we will describe the sources used for each astrophysical tools described above.

4.1 Analysis using SNe Ia data

To perform the cosmological test we will employ the most recent SNe Ia catalog available: the JLA [11]. Its binned compilation shows the same trend as using the full catalog itself, for this reason we will use this reduced sample which can be found in the above reference and explicitly in [23]. This dataset consist of $N_{\rm JLA}=31$ events distributed over the redshift interval 0.01 < z < 1.3. We remark that the covariance matrix of the distance modulus μ used in the binned sample already estimated accounting various statistical and systematic uncertainties. For further discussion see Section 5 in [11, 24].

To perform the statistical analysis of the SNe Ia we employ the distance modules of the JLA sample

$$\mu(z_i, \mu_0) = 5 \log_{10} \left[(1+z) \int_0^z d\tilde{z} E^{-1}(\tilde{z}, \Omega_m; w_0, w_1) \right] + \mu_0$$

where (w_0, w_1) are the free parameters of the model. and compute the best fits by minimizing the quantity

$$\chi_{\text{SN}_{\text{JLA}}}^{2} = \sum_{i=1}^{N_{\text{JLA}}} \frac{\left[\mu(z_{i}, \Omega_{m}; \mu_{0}, w_{0}, w_{1}) - \mu_{\text{obs}}(z_{i})\right]^{2}}{\sigma_{\mu, i}^{2}}$$
(4.1)

where the $\sigma_{\mu,i}^2$ are the measurements variances.

4.2 Analysis using BAO data

We also consider in our analysis the measurements of BAO observations in the galaxy distribution. These observations can contribute important features by comparing the data of the sound horizon today to the sound horizon at the time of recombination (extracted from the CMB anisotropy data). Commonly, the BAO distances are given as a combination of the angular scale and the redshift separation:

$$d_z \equiv \frac{r_s(z_d)}{D_V(z)}, \quad \text{with} \quad r_s(z_d) = \frac{c}{H_0} \int_{z_d}^{\infty} \frac{c_s(z)}{E(z)} dz$$
 (4.2)

where $r_s(z_d)$ is the comoving sound horizon at the baryon dragging epoch, c the light velocity, z_d is the drag epoch redshift and $c_s^2 = c^2/3[1 + (3\Omega_{b0}/4\Omega_{\gamma0})(1+z)^{-1}]$ is the sound speed

with Ω_{b0} and $\Omega_{\gamma 0}$ are the present values of baryon and photon parameters, respectively. By definition the dilation scale is

$$D_V(z, \Omega_m; w_0, w_1) = \left[(1+z)^2 D_A^2 \frac{c z}{H(z, \Omega_m; w_0, w_1)} \right]^{1/3}$$
(4.3)

where D_A is the angular diameter distance:

$$D_A(z, \Omega_m; w_0, w_1) = \frac{1}{1+z} \int_0^z \frac{c \, \mathrm{d}\tilde{z}}{H(\tilde{z}, \Omega_m; w_0, w_1)}$$
(4.4)

Through the comoving sound horizon, the distance ratio d_z is related to the expansion parameter h (defined such that H = 100h) and the physical densities Ω_m and Ω_b .

The BAO distances measurements employed in this paper are compilations of three surveys: $d_z(z=0.106)=0.336\pm0.015$ from 6dFGS [25], $d_z(z=0.35)=0.1126\pm0.0022$ from SDSS [26] and $d_z(z=0.57)=0.0726\pm0.0007$ from BOSS CMASS [27]. Also, we consider three correlated measurements of $d_z(z=0.44)=0.073$, $d_z(z=0.6)=0.0726$ and $d_z(z=0.73)=0.0592$ from the WiggleZ survey [28], with the inverse covariance matrix:

$$\mathbf{C_{WiggleZ}^{-1}} = \begin{pmatrix} 1040.3 & -807.5 & 336.8 \\ -807.5 & 3720.3 & -1551.9 \\ 336.8 & -1551.9 & 2914.9 \end{pmatrix}$$
(4.5)

The χ^2 function for the BAO data can be defined as:

$$\chi_{\text{BAO}}^{2}(\boldsymbol{\theta}) = \mathbf{X}_{\mathbf{BAO}}^{T} \mathbf{C}_{\mathbf{BAO}}^{-1} \mathbf{X}_{\mathbf{BAO}}$$
(4.6)

where $\mathbf{X}_{\mathbf{BAO}}$ is given as

$$\mathbf{X_{BAO}} = \left(\frac{r_s(z_d)}{D_V(z,\Omega_m;w_0,w_1)}\right) - d_z(z)\right) \tag{4.7}$$

Then, the total $\chi^2_{\rm BAO}$ is directly obtained by the sum of the individual quantity by using Equation (4.6) in: $\chi^2_{\rm BAO-total} = \chi^2_{\rm 6dFGS} + \chi^2_{\rm SDSS} + \chi^2_{\rm BOSSCMASS} + \chi^2_{\rm WiggleZ}$.

5 Bayesian Evidence

A Bayesian model selection is a methodology to describe the relationship between the cosmological model, the astrophysical data and the prior information about the free parameters. Using Bayes theorem [32] we can updated the prior model probability to the posterior model probability. However, when we compare models, the *evidence* is used to evaluate the model's evolution using the data available. The evidence is given by

$$\mathcal{E} = \int \mathcal{L}(\theta) P(\theta) d\theta \tag{5.1}$$

where θ is the vector of free parameters, which in our analysis correspond to (w_0, w_a) and $P(\theta)$ is the prior distribution of these parameters. Equation (5.1) can be difficult to calculate due that the integrations can consume to much time when the parametric space is large. Nevertheless, even when several methods exist [33, 34], in this work we applied a nested sampling algorithm [35] which has proven practicable in cosmology applications [36].

We compute the logarithm of the Bayes factor between two models $\mathcal{B}_{ij} = \mathcal{E}_i/\mathcal{E}_j$, where the reference model (\mathcal{E}_i) with highest evidence is the Λ CDM model and impose a flat prior on H_0 . The interpretation scale known as Jeffreys's scale [37], is given as: if $\ln B_{ij} < 1$ there is not significant preference for the model with the highest evidence; if $1 < \ln B_{ij} < 2.5$ the preference is substantial; if $2.5 < \ln B_{ij} < 5$ it is strong; if $\ln B_{ij} > 5$ it is decisive.

6 Results

Our main goal is to investigate the six bidimensional dark energy parameterizations presented in Section 2 and confronting them by using the SNe Ia JLA and BAO datasets in order to explore which has more constraining power and observe whether there is *tension* between these two datasets, which are so far two of the most worthy tools to explore dark energy, and which are anticipated to play an even more preeminent role in the future.

The process of considering dark energy constraints from the combination of SNe Ia JLA and BAO datasets is relevant and useful, as is comparing the individual predictions drawn from each other. This fact does not mean that we are going to completely avoid the use of the CMB analysis; in particular, the selected priors for Ω_m and Ω_b are obtained from a forecast of CMB observations with the Planck mission [10]. The predicted best fits at 68% confidence level are $\Omega_m = 0.3089 \pm 0.0062$ and $\Omega_b = 0.0486 \pm 0.0010$ with our choice for $H_0 = 67.74 \pm 0.46$ km s⁻¹ Mpc⁻¹.

6.1 About the Likelihood and Tension

We will employ the maximum likelihood method in order to determine the best fit values of the parameters w_0 and w_1 for the six parameterizations described. The Λ CDM case can be set with Ω_m as an independent parameter and compute its best fit. The total likelihood for joint data analysis is expressed as the sum of each dataset, i.e.,

$$\chi_{\text{total}}^2 = \chi_{\text{SNe Ia_{JI,A}}}^2 + \chi_{\text{BAO-total}}^2 \tag{6.1}$$

To compare results and test the tension among datasets, we compute the so called σ -distance, d_{σ} , i.e., the distance in units of σ between the best fit points of the SNe Ia, BAO and the total compilation SNe Ia + BAO and the best fit points of each parameterization in comparison to the Λ CDM model. Following [29], the σ -distance is calculated by solving

$$1 - \Gamma(1, |\Delta \chi_{\sigma}^2/2|)/\Gamma(1) = \operatorname{erf}(d_{\sigma}/\sqrt{2})$$
(6.2)

where Γ and erf are the Gamma and error function, respectively. For homogeneity and consistency our 'ruler' is in every case the total χ^2 function Equation (6.1), and our prescription is the following [30]: if we want to calculate the tension between SNe Ia and SNe Ia+BAO and the best fit parameters ([w_0, w_1]) then the previous $\Delta \chi^2_{\sigma}$ will be defined as $\chi^2_{tot}([w_0, w_1]_{\mathbf{SNeIa}+\mathbf{BAO}}) - \chi^2_{tot}([w_0, w_1]_{\mathbf{SNeIa}})$; other cases follow this recipe.

Looking at our results regarding the σ -distances in Tables 1 and 2 we can notice that the *tension* between compilations seems to be reduced when we use the parameterizations that contain z^2 -terms, as the BA and JBP models (see Figures 1 and 2). Is important to address that this tension effect can change depending of the priors Ω_m and Ω_b as it was showed in [30], but even with these changes, the tension remains reduced for the BA and JBP parameterizations.

6.2 About the Figure of Merit (FoM)

In order to statistically compare our results, we compute, first, the Figure of Merit (FoM) as was proposed by the *Dark Energy Task Force* [38], which is generally as the *N*-dimensional volume enclosed by the confidence contours of the free parameters (w_0, w_1) and written as: $\text{FoM}_{(w_0, w_1)} = 1/\sqrt{\det \text{Cov}(w_0, w_1)}$, with $\text{Cov}(w_0, w_1)$ the covariance matrix of the considered theoretical parameters. The FoMs for each dark energy parameterizations are detailed in

Table 3. From these values we notice that the FoM for WP and LC parameterizations are better since they correspond to smaller error ellipse (see Figure 1). Also, we see that BA parameterization shows a large parameter space volume in comparison to the JBP model.

6.3 About the Bayesian Evidence

We estimate the evidence using the algorithm discussed in [36] and run it several times to obtain a distribution of ≈ 100 values to reduce the statistical noise. Then we extract the best value to compute the value of $\ln B_{ij}$, which is reported in Table ?? for each dark energy parameterization. As a result, the $\ln B_{ij}$ values for each dark energy models lies in a region in which Λ CDM is not discounted (1 < $\ln B_{ij}$ < 2.5). These results show a striking evidence in favour of the Λ CDM model. Moreover, BA parameterization display a $\ln B_{ij}$ of around 1% larger than the other parameterizations when SNe Ia+BAO is used.

7 Conclusions

We have presented the study of six bidimensional dark energy parameterizations (Linear, CPL, BA, LC, JBP and WP). All of them were tested using observations from SNe Ia JLA and BAO datasets, together with their combination. Our results indicate that for parameterizations with z^2 -terms in their w(z)-formulation (as BA and JBP models), the tension between these datasets are reduced and their behaviour is $<1\sigma$ compatible with Λ CDM.

Furthermore, for both parameterizations we have $w(z=0)=w_0$, but at high redshifts for BA $w(z\to\infty)=w_0+w_1$ and for JBP $w(z\to\infty)=w_0$, this means that the JBP model can model a dark energy component which has the same equation of state at the present epoch and at high redshift, while for the BA model we can rely on the results only if w_0+w_1 is below zero at the time of decoupling so that dark energy is not relevant for the physics of recombination of the evolution of perturbations up to that epoch. Due to these behaviours we can consider that parameterizations with z^2 -terms are well-behaved and in better agreement with Λ CDM in comparison to other parameterizations where a divergence is present.

Also, the Bayes factor shows striking evidence in favour of the Λ CDM model, but the evidence for the concordance model is substantial with respect to the BA parameterization by around 1% in comparison to the other parameterization. These results seems to be of interest since the bidimensional form of dark energy parameterizations are in better agreement with Λ CDM, wherever higher order parameterizations can be developed.

We remark that these analyses were implemented to perform a complete treatment of selected w(z) parameterizations along the lines of the study of contributions to the matter power spectra [23].

Complementary conclusions are that the use of statistical tools like Akaike Information Criterion (AIC) [39] can help us to discern between dark energy models that display different numbers of free parameters.

Acknowledgments

Celia Escamilla-Rivera is supported by CNPq Brazil Project 502454/2014-8 and would like to thank David Polarski and George Pantazis for their suggestions that improved the paper and Julio Fabris for his insights along these ideas.

References

- [1] Weinberg, S. The Cosmological Constant Problems. 2000, arXiv:astro-ph/0005265.
- [2] Sahni, V.; Starobinsky, A.A. The Case for a positive cosmological Lambda term. *Int. J. Mod. Phys. D* **2000**, 9, 373–443.
- [3] Feng, L.; Lu,T. A new equation of state for dark energy model. *J. Cosmol. Astropart. Phys.* **2011**, *2011*, 034.
- [4] Stefancic, H. Equation of state description of the dark energy transition between quintessence and phantom regimes. J. Phys. Conf. Ser. 2006, 39, 182.
- [5] Wang, Y.; Tegmark, M. Uncorrelated measurements of the cosmic expansion history and dark energy from supernovae. Phys. Rev. D 2005, 71, 103513.
- [6] Barboza, E.M.; Alcaniz, J.S.; Zhu, Z.-H.; Silva, R. A generalized equation of state for dark energy. *Phys. Rev. D* **2009**, *80*, 043521.
- [7] Pantazis, G.; Nesseris, S.; Perivolaropoulos, L. Comparison of thawing and freezing dark energy parametrizations. *Phys. Rev. D* **2016**, *93*, 103503.
- [8] Wang, Y. Figure of merit for dark energy constraints from current observational data. Phys. Rev. D 2008, 77, 123525.
- [9] Jassal, H.K.; Bagla, J.S.; Padmanabhan, T. WMAP constraints on low redshift evolution of dark energy. *Mon. Not. Roy. Astron. Soc.* **2005**, *356*, L11.
- [10] Ade, P.A.R.; Aghanim, N.; Arnaud, M.; Ashdown, M.; Aumont, J.; Baccigalupi, C.; Banday, A.J.; Barreiro, R.B.; Bartlett, J.G.; Bartolo, N.; et al. Planck 2015 Results. XIII. Cosmological Parameters. 2015, arXiv:astro-ph.CO/1502.01589.
- [11] Betoule, M.; Kessler, R.; Guy, J.; Mosher, J.; Hardin, D.; Biswas, R.; Astier, P.; El-Hage, P.; Konig, M.; Kuhlmann, S.; et al. Improved cosmological constraints from a joint analysis of the SDSS-II and SNLS supernova samples. *Astron. Astrophys.* **2014**, *568*, A22.
- [12] Busca, N.G.; Delubac, T.; Rich, J.; Bailey, S.; Font-Ribera, A.; Kirkby, D.; Le Goff, J.-M.; Pieri, M.M.; Slosar, A.; Aubourg, É.; et al. Baryon Acoustic Oscillations in the Ly-α forest of BOSS quasars. Astron. Astrophys. 2013, 552, A96.
- [13] Lazkoz, R.; Nesseris S.; Perivolaropoulos, L. Exploring Cosmological Expansion Parametrizations with the Gold SnIa Dataset. *J. Cosmol. Astropart. Phys.* **2005**, 2005, 010.
- [14] Peebles, P.J.E.; Ratra, B. The Cosmological constant and dark energy. Rev. Mod. Phys. 2003, 75, 559–606.
- [15] Huterer, D.; Turner, M.S. Probing the dark energy: Methods and strategies. *Phys. Rev. D* **2001**, *64*, 123527.
- [16] Weller, J.; Albrecht, A. Future supernovae observations as a probe of dark energy. Phys. Rev. D 2002, 65, 103512.
- [17] Wang, F.Y.; Dai, Z.G. Constraining Dark Energy and Cosmological Transition Redshift with Type Ia Supernovae. *Chin. J. Astron. Astrophys.* **2006**, *6*, 561.
- [18] Linder, E.V. The dynamics of quintessence, The quintessence of dynamics. *Gen. Rel. Grav.* **2008**, 40, 329–356.
- [19] Chevallier, M.; Polarski, D. Accelerating universes with scaling dark matter. Int. J. Mod. Phys. D 2001, 10, 213–223.
- [20] Barboza, E.M., Jr.; Alcaniz, J.S. A parametric model for dark energy. Phys. Lett. B 2008, 666, 415–419.

- [21] Wetterich, C. Phenomenological parameterization of quintessence. *Phys. Lett. B* **2004**, *594*, 17–22.
- [22] Wetterich, C. Cosmology with Varying Scales and Couplings. 2003, arXiv:hep-ph/0302116.
- [23] Escamilla-Rivera, C.; Casarini, L.; Fabris, J.C.; Alcaniz, J.S. Linear and non-linear perturbations in dark energy models. 2016, arXiv:1605.01475.
- [24] Conley, A.; Guy, J.; Sullivan, M.; Regnault, N.; Astier, P.; Balland, C.; Basa, S.; Carlberg, R.G.; Fouchez, D.; Hardin, D.; et al. Supernova Constraints and Systematic Uncertainties from the First 3 Years of the Supernova Legacy Survey. *Astrophys. J. Suppl.* **2011**, *192*, 1.
- [25] Beutler, F.; Blake, C.; Colless, M.; Jones, D.H.; Staveley-Smith, L.; Campbell, L.; Parker, Q.; Saunders, W.; Watson, F.; et al. The 6dF Galaxy Survey: Baryon Acoustic Oscillations and the Local Hubble Constant. *Mon. Not. Roy. Astron. Soc.* **2011**, *416*, 3017–3032.
- [26] Anderson, L.; Aubourg, É; Bailey, S.; Beutler, F.; Bhardwaj, V.; Blanton, M.; Bolton, A.S.; Brinkmann, J.; Brownstein, J.R.; Burden, A.; et al. The clustering of galaxies in the SDSS-III Baryon Oscillation Spectroscopic Survey: baryon acoustic oscillations in the Data Releases 10 and 11 Galaxy samples. *Mon. Not. Roy. Astron. Soc.* **2014**, *441*, 24–62.
- [27] Xu, X.; Padmanabhan, N.; Eisenstein, D.J.; Mehta, K.T.; Cuesta, A.J. A 2% Distance to z=0.35 by reconstructing baryon acoustic oscillations–II: Fitting techniques. *Mon. Not. Roy. Astron. Soc.* **2012**, 427, 2146-2167.
- [28] Blake, C.; Brough, S.; Colless, M.; Contreras, C.; Couch, W.; Croom, S.; Croton, D.; Davis, T.M.; Drinkwater, M.J.; Forster, K.; et al. The WiggleZ Dark Energy Survey: Joint measurements of the expansion and growth history at z < 1. *Mon. Not. Roy. Astron. Soc.* **2012**, 425, 405–414.
- [29] Press W.H.; Teukolsky A.; Vetterling W.; Flannery B. Numerical Recipes, 3rd, ed.; Cambridge Press: New York, USA, 1994.
- [30] Escamilla-Rivera, C.; Lazkoz, R.; Salzano, V.; Sendra, I. Tension between SN and BAO: Current status and future forecasts. J. Cosmol. Astropart. Phys. 2011, doi:10.1088/1475-7516/2011/09/003.
- [31] Burigana, C.; Destri, C.; de Vega, H.J.; Gruppuso, A.; Mandolesi, N.; Natoli, P.; Sanchez, N.G. Forecast for the Planck precision on the tensor to scalar ratio and other cosmological parameters. *Astrophys. J.* **2010**, *724*, 588.
- [32] Bayes, R.T. An essay toward solving a problem in the doctrine of chances. *Phil. Trans. R. Soc. Lond.* **1764**, *53*, 370–418.
- [33] Gregory, P. Bayesian Logical Data Analysis for the Physical Sciences; Cambridge University Press: New York, USA, 2005.
- [34] Trotta, R. Applications of Bayesian model selection to cosmological parameters. *Mon. Not. Roy. Astron. Soc.* **2007**, *378*, 72–82.
- [35] Skilling J. Bayesian annal 1, 2006, 833. http://www.mrao.cam.ac.uk/~steve/maxent2009/images/skilling.pdf
- [36] Liddle, A.R.; Mukherjee, P.; Parkinson, D.; Wang, Y. Present and future evidence for evolving dark energy. *Phys. Rev. D* **2006**, *74*, 123506.
- [37] Jeffreys, H. *Theory of Probability*, 3rd ed.; Oxford University Press: Oxford, United Kingdom. 1998.
- [38] Albrecht, A.; Amendola, L.; Bernstein, G.; Clowe, D.; Eisenstein, D.; Guzzo, L.; Hirata, C.; Huterer, D.; Kirshner, R.; Kolb, E.; et al. Findings of the Joint Dark Energy Mission Figure of Merit Science Working Group. **2009**, arXiv:0901.0721

[39] Liddle, A.R. How many cosmological parameters? Mon. Not. Roy. Astron. Soc. 2004, 351, L49–L53.

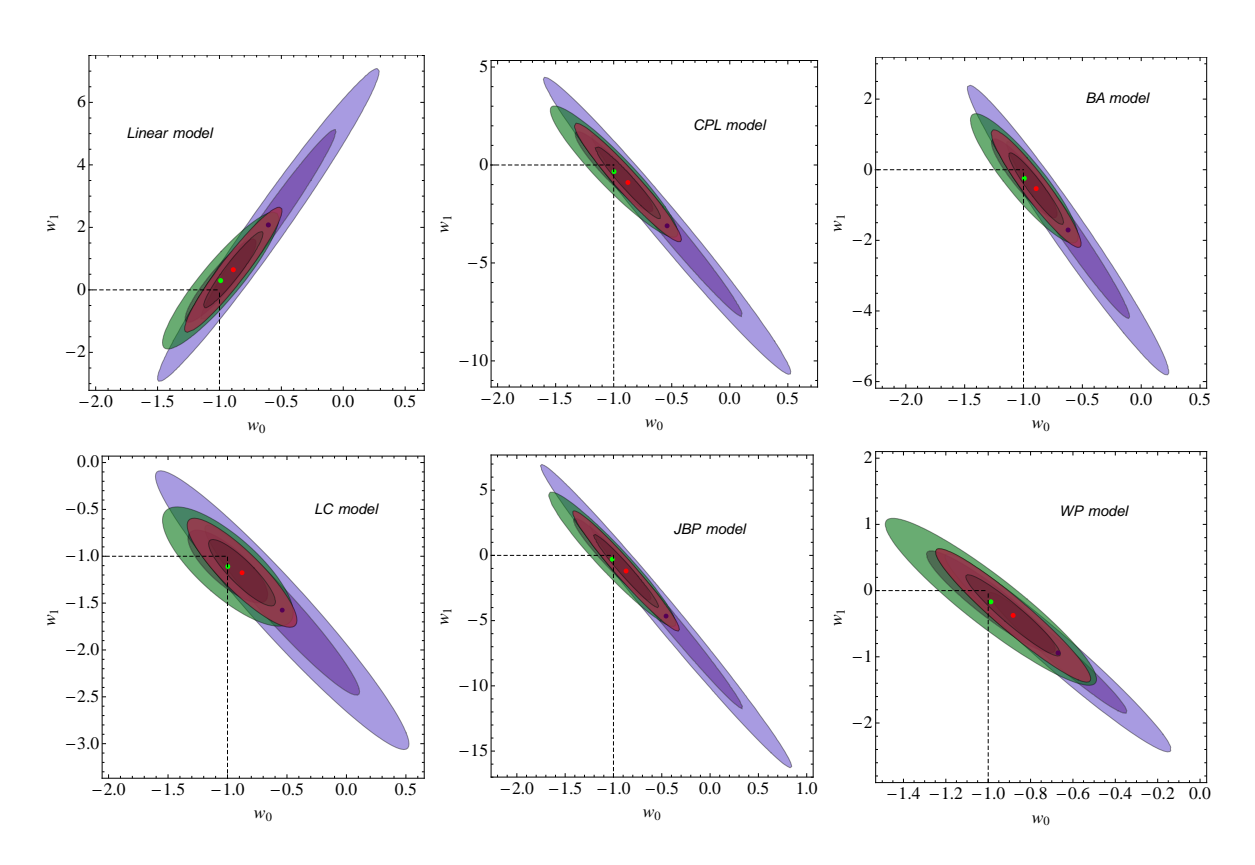


Figure 1. 1 and 2σ confidence contours for dark energy parameterizations. In supernovae Joint Lightcurve Analysis (SNe Ia JLA) is represented by the green region, the baryon acoustic oscillations (BAO) by the purple region and SNe Ia JLA+BAO by the red region. The best fits are indicated by the points for each sample, respectively. The point where the dashed line cross indicates the concordance model (Λ CDM).

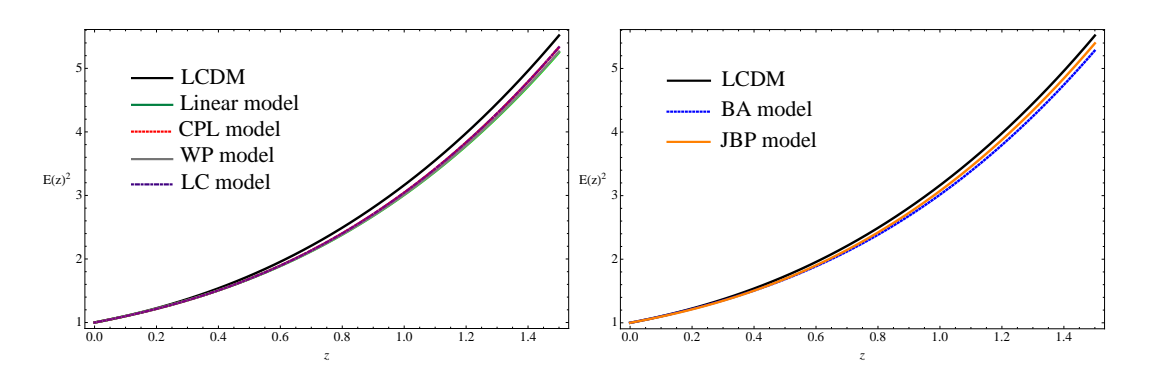


Figure 2. $E(z)^2$ evolution function for each dark energy parameterizations. We use the best fit obtained in each parameterizations with the SNe Ia JLA+BAO joined dataset. *Left:* Evolution of Equation (3.1) and the bidimensional dark energy parameterizations Equations (3.3), (3.5) and (3.13). *Right:* Evolution of the Equations (3.1) and the bidimensional dark energy parameterizations (3.7)–(3.11) (with z^2 -terms in w(z)).

Model	Parameterisation	$d_{\sigma}^{\Lambda CDM}$	Best Fit Parameters using SNe Ia JLA data
LCDM	('')0[111(- 1 '') 1 (111)]	_	$\Omega_m = 0.295 \pm 0.034$
Linear	$H^{2}(z) = H_{0}^{2} [\Omega_{m}(1+z)^{3} + (1-\Omega_{m})(1+z)^{3(1+w_{0}+w_{1})}e^{-3w_{1}z}]$	0.285	$w_0 = -0.991 \pm 0.036, \ w_1 = 0.297 \pm 0.779$
CPL	$H^{2}(z) = H_{0}^{2}[\Omega_{m}(1+z)^{3} + (1-\Omega_{m})(1+z)^{3(1+w_{0}+w_{1})}]$		
	$\times e^{\frac{-3w_1z}{1+z}}]$	0.258	$w_0 = -0.997 \pm 0.049, \ w_1 = -0.337 \pm 1.822$
BA	$H^{2}(z) = H_{0}^{2} [\Omega_{m}(1+z)^{3} + (1-\Omega_{m})(1+z)^{3(1+w_{0})}]$		
	$\times (1+z^2)^{3w_1/2}$	0.243	$w_0 = -0.993 \pm 0.034, \ w_1 = -0.245 \pm 0.545$
LC	$H^{2}(z) = H_{0}^{2} [\Omega_{m}(1+z)^{3} + (1-\Omega_{m})(1+z)^{3(1-2w_{0}+3w_{0.5})}]$		
	$\times e^{\left[\frac{9(w_0-w_{0.5})z}{1+z}\right]}]$	0.258	$w_0 = -0.997 \pm 0.049, \ w_{0.5} = -1.109 \pm 0.066$
JBP	$H^{2}(z) = H_{0}^{2}[\Omega_{m}(1+z)^{3} + (1-\Omega_{m})(1+z)^{3(1+w_{0})}]$		
	$\times e^{\frac{3w_1z^2}{2(1+z)^2}}]$	0.236	$w_0 = -1.013 \pm 0.070, \ w_1 = -0.295 \pm 4.306$
WP	$H^{2}(z) = H_{0}^{2} \left\{ \Omega_{m}(1+z)^{3} + (1-\Omega_{m})(1+z)^{3} \left[1 + \frac{w_{0}}{1+w_{1}\ln(1+z)} \right] \right\}$	0.278	$w_0 = -0.987 \pm 0.040, \ w_1 = -0.169 \pm 0.258$

Table 1. Dark energy parameterisations with best fits and σ -distances values using SNe Ia JLA data.

Model	Best Fit Parameters using BAO data	$d_{\sigma}^{\Lambda CDM}$	Best Fit Parameters using SNe Ia JLA+BAO data	$d_{\sigma_{Total}}^{\Lambda CDM}$
Linear	$w_0 = -0.605 \pm 0.130, \ w_1 = 2.078 \pm 4.063$	0.610	$w_0 = -0.888 \pm 0.025, \ w_1 = 0.645 \pm 0.650$	0.380
CPL	$w_0 = -0.540 \pm 0.184, \ w_1 = -3.105 \pm 9.327$	0.594	$w_0 = -0.878 \pm 0.034, \ w_1 = -0.894 \pm 1.487$	0.323
BA	$w_0 = -0.621 \pm 0.119, \ w_1 = -1.707 \pm 2.731$	0.600	$w_0 = -0.892 \pm 0.024, \ w_1 = -0.535 \pm 0.450$	0.316
LC	$w_0 = -0.540 \pm 0.184, \ w_{0.5} = -1.575 \pm 0.359$	0.594	$w_0 = -0.878 \pm 0.034, \ w_{0.5} = -1.175 \pm 0.054$	> 1
JBP	$w_0 = -0.456 \pm 0.274, \ w_1 = -4.653 \pm 21.910$	0.569	$w_0 = -0.869 \pm 0.049, \ w_1 = -1.196 \pm 3.441$	0.257
WP	$w_0 = -0.670 \pm 0.046, \ w_1 = -0.941 \pm 0.363$	0.626	$w_0 = -0.882 \pm 0.022, \ w_1 = -0.375 \pm 0.165$	0.386

Table 2. Dark energy parameterisations with best fits and σ -distances values using BAO and the combining samples.

Table 3. Values of the Figure of Merit for each parameterisation

Model	FoM			
	SNe Ia JLA	BAO	SNe Ia+BAO	
Linear	14.203	7.015	23.657	
CPL	9.312	4.631	15.681	
LC	27.936	13.893	47.043	
BA	16.981	8.555	28.437	
JBP	6.076	3.024	10.337	
WP	26.208	33.996	53.677	

Table 4. Values of Bayes factor for each parameterisation.

	Model	Bayes factor $\ln B_{ij}$			
		SNe Ia JLA	BAO	SNe Ia JLA+BAO	
ſ	Linear	1.904	1.897	1.857	
İ	CPL	1.912	1.903	1.875	
İ	LC	1.912	1.903	1.875	
İ	BA	1.921	1.921	1.921	
İ	$_{ m JBP}$	1.918	1.912	1.854	
ı	WP	1.906	1.891	1.855	